

UNIFIED TREATMENT OF HADRONIC PROCESSES  
 INVOLVING HIGH MASS VIRTUAL PHOTONS\*

John Harte

Stanford Linear Accelerator Center  
 Stanford University, Stanford, California 94305

and

Yale University, New Haven, Connecticut 06520

ABSTRACT

A unified treatment of the three processes: (I) lepton + proton  $\rightarrow$  lepton + hadrons, (II) proton + proton  $\rightarrow$  lepton pair + hadrons, (III) lepton pair  $\rightarrow$  hadrons is presented. Our dynamical model is an off-mass-shell bootstrap theory of the hadrons. We show that the model predicts slow  $q^2$  (photon mass squared) variation of the differential cross sections for processes I and II in spite of the fact that the model requires the elastic and quasi-elastic hadronic form factors to decrease faster than any power in  $q^2$ . The cross section for process III, however, is predicted to decrease rapidly in  $q^2$  and to violate the scaling law observed for process I. More detailed predictions of multiplicities and angular distributions of the final states are made, as well as the surprising predictions that for large  $q^2$ , the ratio

$$\frac{d\sigma(pp \rightarrow pp + \text{lepton pair})}{dq^2} \bigg/ \frac{d\sigma(pp \rightarrow pp\pi + \text{lepton pair})}{dq^2}$$

for process II and the ratio

$$\sigma(\text{lepton pair} \rightarrow \bar{p}p) / \sigma(\text{lepton pair} \rightarrow \pi^0 + \text{real photon})$$

for process III should both approach zero. The latter ratio should be comparable to 1 for  $q^2 \approx 6 \text{ BeV}^2$ .

---

\* Work supported by the U. S. Atomic Energy Commission.

## I. INTRODUCTION

An exciting new realm of high energy physics has been opened with the advent of experimental access to the deep inelastic region in electron-proton scattering.<sup>1</sup> Future experiments involving virtual photons and hadrons in regions which are kinematically inaccessible in electron-proton scattering, such as lepton pair production in proton-proton scattering or lepton pair annihilation into hadrons, can be expected to provide still further information about the strong interactions. The purpose of this article is to give a unified treatment of these processes within the framework of an off-mass-shell bootstrap theory.<sup>2</sup> The hadrons in our bootstrap are described as infinitely composite particles and in Ref. 2 we derived within the model a tree theorem for the asymptotic form of the n-particle scattering amplitudes satisfying exact unitarity and crossing symmetry. This theory has been successful in correlating the elastic nucleon form factors at large momentum transfers and wide angle elastic proton-proton scattering.<sup>3</sup>

We shall study here the three processes shown in Fig. 1. Figure 1a shows the inelastic electron-proton scattering process which involves the scattering of a virtual space-like photon off a proton; Fig. 1b illustrates proton-proton scattering with the production of a time-like photon which subsequently creates a lepton pair; and Fig. 1c shows lepton pair annihilation into a time-like photon which subsequently "decays" into the final state hadrons. We shall refer to these three processes as process I, II and III, respectively.

Among the features of these processes that we shall be interested in here are the  $q^2$  dependence of the differential cross sections, the multiplicities of final state hadrons and the angular distributions. We shall also discuss briefly the scaling law<sup>4</sup> which, for process I, states that  $\nu W_2$  and  $W_1$  are functions only of the dimensionless variable  $\omega = 2M_N \nu / Q^2$  where  $\nu$  is the energy of the

photon in the lab system,  $\sqrt{q^2} = \sqrt{-Q^2}$  is the mass of the photon,  $M_N$  is the nucleon mass, and the  $W_i$  are the structure functions for the process.

Of primary interest to us here is the following question: "Why is the differential cross section for process I slowly varying in  $Q^2$  in the deep inelastic region<sup>1</sup> whereas the elastic nucleon form factor is quite rapidly decreasing?<sup>5</sup>" We show here that our bootstrap theory provides a natural answer to this question, and furthermore allows us to predict the  $Q^2$  dependence of processes II and III, as well as the expected multiplicities and the angular distributions of the final state hadrons.

## II. THE DYNAMICAL MODEL

The result from the bootstrap model of Ref. 2 that we shall use over and over here is an explicit expression for the "vertex" shown in Fig. 2 in the asymptotic limit  $|q^2| \rightarrow \infty$ . In this figure,  $q^2$  is the square of the mass of the virtual photon and the lines with total momenta  $p$  and  $p' = p + q$  may refer to single particle or multiparticle states. If the lines  $p$  and  $p'$  refer to single-particle states, then the bootstrap model predicts that the vertex function  $\Gamma(q^2, p^2, p'^2)$  is given, for large  $q^2$ , by

$$\Gamma(q^2, p^2, p'^2) \approx e^{-a g(q^2) g(p^2) g(p'^2)} \quad (1)$$

where

$$\frac{\log q^2}{g(q^2)} \xrightarrow{q \rightarrow \infty} 0, \quad g(q^2) \leq (q^2)^{1/2} \quad (2)$$

and

$$g(0) = 0, \quad (3)$$

and  $a$  is a universal constant independent of the types of particles coupling at the vertex. In Ref. 2 we gave further arguments to suggest that for  $q^2 \rightarrow \infty$ ,

$$g(q^2) \rightarrow (q^2)^{1/4} \quad (4)$$

but we shall only assume Eqs. (1), (2), and (3) here. Equations (1) and (2) imply that for on-shell hadrons, the vertex function decreases faster than any power in  $q^2$ . Equation (3), which is crucial to our model, implies that the vertex connecting a high mass photon to a line of zero virtual mass or a real massless particle does not decrease faster than any power in  $q^2$ . In other words, a massless particle must appear as an elementary, or point-like particle, in the sense that its form factor is not rapidly decreasing. Equation (1) is derived in Ref. 2 up to a possible multiplicative term with power dependence on the invariant variables.

For the case in which  $p$  and  $p'$  refer to multiparticle states, the  $q^2$  dependence of the amplitude for the process shown in Fig. 2 is given by the composite-tree graph theorem of Ref. 2, which we now summarize. First replace the diagram in Fig. 2 with the sum of all tree graphs which are topologically possible with trilinear couplings in such a way that only stable hadron states appear as external lines. Then replace each vertex in each graph by the vertex function in Eq. (1). In the limit  $q^2 \rightarrow \infty$ , the tree theorem states that this prescription gives the correct  $q^2$  dependence of the process.

This result, which is shown in Ref. 2 to be true more generally for all  $n$ -particle scattering amplitudes follows from crossing symmetry and exact unitarity through the use of off-mass-shell equations which enforce the latter condition via the Landau-Cutkosky rules. One consequence of this theorem is a result for the elastic proton-proton scattering amplitude: For large  $|s|$ ,  $|t|$ , and  $|u|$ , the tree theorems relates the scattering amplitude  $A(s,t,u)$  to the sum of the squares of the nucleon form factor in the  $s$ ,  $t$ , and  $u$  channels, each of the three terms being a contribution from one of the three tree graphs that can be drawn for a two-body scattering process. This justification and refinement of the Wu-Yang idea is shown in Ref. 3 to be in excellent agreement with the wide-angle  $p$ - $p$  scattering data.

We emphasize that the tree graphs employed here are not Feynman graphs but rather convenient devices for keeping track of the variables in a many particle amplitude. The internal lines do not correspond to single particle states but simply to the generalized momentum transfers which are topologically permitted in a many particle amplitude.

In order to apply the above results to the virtual-photon processes, we make use of the tree theorem and Eqs. (1), (2), and (3) to conclude that if in the tree decomposition of the process under consideration, there is a graph in which a line with zero virtual mass connects to the photon vertex then the contribution of that graph to the differential cross section does not decrease rapidly in  $q^2$  and thus, for large  $q^2$ , may give the dominant contribution. If, on the other hand, no zero mass line can connect to the photon vertex because of kinematical restrictions, then the differential cross section must decrease faster than any power in  $q^2$ . An example of a process in which the latter situation occurs is, of course, just elastic electron-proton scattering. In the following three sections we treat each of the three processes shown in Fig. 1 from the point of view outlined above.

### III. DEEP INELASTIC ELECTRON-PROTON SCATTERING

We begin the analysis of process I by making the tree graph decomposition shown in Fig. 3a. The heavy lines do not refer to single particle states but to states of definite momentum with an unspecified number of particles, whereas the external straight lines refer to initial and final state stable hadrons.

Let us next determine the contribution of each of these tree graphs to the differential cross section

$$\frac{d^2\sigma}{dq^2 d\nu} = \frac{E'}{E} \frac{4\pi\alpha^2}{q^4} \left[ W_2(q^2, \nu) \cos^2 \frac{\theta}{2} + 2W_1(q^2, \nu) \sin^2 \frac{\theta}{2} \right] \quad (5)$$

where  $E$  and  $E'$  are the initial and final electron energies,  $\theta$  is the electron scattering angle,  $\nu = E - E'$  and  $q^2$  vs the invariant photon mass squared.

We introduce the c. m. energy, of the  $\gamma$ -p system,  $\sqrt{s}$ , which is related to  $\nu$  and  $q^2$  by

$$s = 2M_N\nu - Q^2 + M_N^2 \quad (6)$$

where  $Q^2 = -q^2$ . Then the contribution coming from the first tree graph on the right-hand side in Fig. 3a, to the structure functions  $W_1$  and  $W_2$ , has a  $Q^2$  dependence of the form

$$W_i(Q^2, s) \simeq e^{-2ag(q^2)} g(s) g(M_N^2) \quad (7)$$

since in this tree graph a line with four momentum squared equal to  $s$  couples directly to the photon vertex. Now  $s$  is large in the deep inelastic region characterized by  $\omega = \frac{2M_N\nu}{Q^2} > 1$  and  $Q^2 \rightarrow \infty$ , and therefore this contribution clearly falls off rapidly in  $Q^2$  because of Eq. (2) and is expected to be negligible.

Consider next all tree graphs of the form of the second term on the right-hand side of Fig. 3a, that is all tree graphs characterized by a peripheral mechanism for particle production. The most general such tree graph is shown in Fig. 3b; the two vertices indicated by open circles can be further decomposed into trees but that is unnecessary for our purposes. We label the invariant mass of the top cluster of hadrons closest to the photon vertex by  $M_2$  and the invariant mass of the other cluster by  $M_1$ .

We next determine whether this decomposition can be made in such a way that the invariant momentum transfer,  $t$ , between the photon and the top cluster of hadrons in the tree graph can vanish in the physical region. To determine this we calculate the boundary,  $t_0$ , of the physical region in  $t$ , which can easily be shown to be

$$t_0 \simeq \frac{M_N^2}{\omega} - \frac{M_1^2}{\omega - 1} \quad (8)$$

in the limit of large  $Q^2$  and  $\omega > 1$ . Clearly the condition that  $t = 0$  lies in the physical region is equivalent to the condition  $t_0 \geq 0$  and this imposes the constraint

$$M_1^2 \leq M_N^2 \frac{\omega-1}{\omega} \quad (9)$$

Let us first assume this constraint is satisfied. Then  $t = 0$  lies in the physical region and these tree graphs will give a contribution to

$$\frac{d^3\sigma}{dq^2 d\nu dt}$$

which, according to the tree theorem, will have a  $Q^2$  dependence of the form

$$\bar{W}_i(q^2, \nu, t) \approx F e^{-ag(q^2)g(t)g(M_2^2)} \quad (10)$$

where the  $\bar{W}_i(q^2, \nu, t)$  are related to  $d^3\sigma/dq^2 d\nu dt$  in the same way that the  $W_i(q^2, \nu)$  are related to  $d^2\sigma/dq^2 d\nu$ , and where  $F$  is an undetermined function of  $\nu$  and  $t$ . Since the point  $t = 0$  lies in the physical region, an application of Eq. (3) gives us the result that the structure functions

$$W_i(q^2, \nu) = \int_{t_0}^{t_{\max}} dt W_i(q^2, \nu, t) \quad (11)$$

are slowly varying<sup>6</sup> in  $Q^2$ .

Thus we can explain the rapid (faster than any inverse power) decrease of the elastic nucleon form factor, for which there is no decomposition corresponding to Fig. 3b, and at the same time understand the slow  $Q^2$  dependence of the structure functions for process I, in the deep inelastic region. The mechanism which allows the behavior is the peripheral contribution of Fig. 3b coupled with Eqs. (1), (2), and (3) which state that the form factor of a massless particle does not decrease exponentially. This result is thus related to the suggestion of Harari<sup>7</sup> that the Pomeron exchange contribution to virtual Compton scattering

might produce the slow  $Q^2$  dependence of the  $W_i$ . However, we have here a dynamical origin for this behavior in Eqs. (1), (2), and (3) whereas in the Regge exchange model one has, in addition, to invoke scaling. Our model, unfortunately, says nothing about scaling for process I, although it is not inconsistent with the scaling law.

More detailed information about process I can be obtained from Eq. (8) or Eq. (9). The most obvious restriction is that the condition  $t_0 \geq 0$  forces  $M_1^2$  to be less than  $M_N^2$  so that the outgoing proton must be observed coming from the upper vertex. Therefore, since the dominant contribution comes from  $t \sim 0$ , the proton must be observed going nearly forward relative to the incident photon, in the c. m. system and the lab system.

For an arbitrary final state in the configuration depicted in Fig. 3b, the cosine of the lab angle,  $\theta_L$ , between the incident photon and the outgoing mesons with invariant mass  $M_1$  emitted at the lower vertex is given, at  $t = 0$ , by

$$\cos \theta_L = \frac{M_N(Q^2 + M_2^2) + \nu(M_1^2 - M_N^2)}{\sqrt{\nu^2 + Q^2}(M_N^2 - M_1^2)} \quad (12)$$

Hence, for particular final state, Eq. (12) provides a value of  $\cos \theta_L$  about which the meson production rate must be strongly peaked because of the expected exponential decrease away from  $t = 0$ . Taking  $Q^2, M_N \nu \gg M_N^2, M_1^2 = M_\pi^2, M_2^2 = M_N^2$  and  $\omega \equiv 2 M_N \nu / Q^2 = 2$ , as an example, we obtain a value

$$\cos \theta_L = 0 \quad (13)$$

So if one selects data corresponding to  $\omega = 2$ , a strong peaking of the pion angular distribution about  $90^\circ$  is expected. In addition, for this particular case of a  $\pi N$  final state, the magnitude of the pion lab momentum,  $\vec{p}_\pi$ , is expected to peak at  $|\vec{p}_\pi| \simeq M_N/2$  since the momentum transfer,  $t_1$  can be written

$$t = M_\pi^2 + M_N^2 - 2M_N \sqrt{p_\pi^2 + M_\pi^2} \quad (14)$$



The outgoing proton is expected to emerge in the forward direction with a lab momentum  $|\vec{p}_N| \approx \nu$ .

Equation (9) forces further restrictions on the multiplicities of the produced particles. As the multiplicities of final state particles produced at the lower vertex increase,  $M_1^2$  must increase, until for large enough  $M_1^2$ ,  $t_0$  becomes negative and the amplitude decreases rapidly in  $Q^2$ . For example, the condition that there be a significant  $p + 2\pi$  final state with the two pions resulting from  $\rho$ -production at the lower vertex is, from Eq. (9),

$$\omega \equiv \frac{2M_N\nu}{Q^2} \geq \frac{M_N^2}{M_N^2 - M_\rho^2} \approx 2.75, \quad (15)$$

Similarly, the condition for strange particle production, for example, a  $\Sigma K$  final state, is

$$\omega \equiv \frac{2M_N\nu}{Q^2} \geq \frac{M_N^2}{M_N^2 - M_K^2} \approx 1.40 \quad (16)$$

For values of  $\omega$  smaller than 2.75 and 1.40, the amplitudes for  $\rho$  and  $K$  production, respectively, should be quite small for large  $Q^2$  although there is still the possibility for them to be produced at the upper vertex.

Finally, we see from Eq. (8) that for  $\omega$  sufficiently close to 1, even the minimum possible value  $M_1^2 = M_\pi^2$ , forces  $t_0$  to be negative and the amplitude for all final states must be rapidly decreasing in  $Q^2$  for large  $Q^2$ . This predicted precipitous decrease of the  $W_i$  occurs for

$$\omega \leq \omega_0 \approx \frac{1}{1 - M_\pi^2/M_N^2} \quad (17)$$

which implies, by Eq. (6),

$$s > s_0 \approx \frac{2M_\pi^2\nu}{M_N} \quad (18)$$

Now in order for this effect to be observable above the resonances, which should also give rise to rapidly decreasing structure functions for large  $Q^2$ , we require

$$s_0 > s_R \quad (19)$$

where  $s_R$  characterizes the upper end of the resonance-dominated region in the variable  $s$ . Note, further, that in the region characterized by Eq. (17) and Eq. (18) the scaling law must break down because the exponential in Eq. (1) does not scale.

This breakdown of scaling and rapid decrease of the differential cross section in  $Q^2$  occurs in a region characterized by a value of  $s$  which grows with  $\nu$ , whereas scaling would break down in the region  $s \leq s_R$  if only the resonance contribution destroyed the scaling law. Approximating  $s_R$  by  $4M_N^2$ , we obtain

$$\nu \geq \frac{2M_N^3}{M_\pi^2} \quad (20)$$

so that this effect is unfortunately not observable at presently available energies.

The process  $e\pi \rightarrow e + \text{hadrons}$  offers an even more dramatic (although no more practical!) example of this effect. For this process, Eq. (9) is replaced by  $M_1^2 \leq M_\pi^2 \left(\frac{\omega-1}{\omega}\right)$  so that no final state is compatible with a  $t = 0$  line connecting to the photon vertex and thus, for all values of  $\omega$ , the differential cross section is rapidly decreasing in  $Q^2$  and violates the scaling law. Thus our model is in fundamental disagreement with the model of Ref. 7 in which the Pomeron exchange contribution to virtual Compton scattering off pions would result in a differential cross section for the process  $e\pi \rightarrow e + \text{hadrons}$  which would be essentially similar to that for  $ep \rightarrow e + \text{hadrons}$ .

#### IV. VIRTUAL PHOTON PRODUCTION IN $pp$ SCATTERING

The preceding discussion is easily extended to process II. As before, we decompose the diagram in Fig. 1b into the tree graphs in Fig. 4a. The first

tree graph on the right-hand side of Fig. 4a is clearly negligible at large  $s$  because it will decrease faster than any power in  $s$ . Let us look next at the second and third tree graphs in the figure.

These tree graphs are of the general form of the graph illustrated in Fig. 4b, in which the photon is emitted along with a group of hadrons at the top vertex labeled with an invariant mass  $M_2$ , and a group of hadrons is emitted at the lower vertex, with invariant mass  $M_1$ . The open circles in Fig. 4b can, of course, be further decomposed into tree graphs. For example, the second graph on the right-hand side of Fig. 4a can be considered to be of this form with  $M_2^2 = q^2$ , and all the hadrons emitted at the lower vertex.

We define  $t$  to be the momentum transfer between one of the protons and the group of particles labeled with invariant mass  $M_1$  in the figure. In analogy with the arguments of the preceding sections, then, we can expect the cross section to be a slowly varying function of  $q^2$  for  $t \approx 0$ .

As before we define  $t = t_0$  to be the edge of the physical region, and find, for sufficiently large  $s$  and large  $q^2$ , that

$$t_0 = \frac{M_N^2}{c} - \frac{M_1^2}{c-1} \quad (21)$$

where

$$c = \frac{s}{M_2^2} \quad (22)$$

The quantity  $c$ , which must satisfy  $c \geq 1$ , is clearly playing the same role here as did the variable  $\omega$  in Eq. (8). If  $M_1^2 \geq M_N^2$ ,  $t_0$  is always negative and the cross section must be rapidly decreasing in  $q^2$ . If  $M_1^2$  is sufficiently small, then  $t_0 \geq 0$  and the differential cross section should be slowly varying in  $q^2$ . The photon propagator will give rise to a  $1/q^4$  dependence of the differential cross sections, and the experimental indications<sup>6</sup> are that no other appreciable  $q^2$  dependence should be present. Thus the photon and the two

protons must emerge, together, at the top vertex and a particle or particles with invariant mass  $M_1^2 \leq M_N^2$  (i. e. , mesons) must emerge from the other. The photon and the nucleons will be observed going in one direction in the c. m. system and the lighter particle or group of particles emerging in the opposite direction.

More interesting is the observation that at least one meson must be emitted along with the photon and two protons in the final state. This prediction is a consequence of the fact that the process  $pp \rightarrow \gamma pp$  cannot occur, for  $q^2 \geq M_N^2$ , in a tree configuration with a line of zero virtual mass connecting to the photon.

Therefore the ratio

$$\frac{\left. \frac{d^2\sigma}{d\Omega dq^2} \right|_{pp \rightarrow \gamma pp}}{\left. \frac{d^2\sigma}{d\Omega dq^2} \right|_{pp \rightarrow \gamma pp \pi}} \quad (23)$$

must go to zero faster than any power of  $q^2$ .

Finally, interesting statements can be made about the values of  $q^2$ , for fixed  $s$ , at which the production of particular final states is inhibited because their presence does not allow  $t = 0$  to be in the physical region. For the case  $s = 60$  ( $\text{BeV}^2$ ) one can easily show from Eqs. (21) and (22) that  $\rho$ -production at the lower vertex in Fig. 5b is inhibited for  $q^2 > 8 \text{ BeV}^2$ , K production is inhibited for  $q^2 \geq 23 \text{ BeV}^2$  and  $\pi$  production (and therefore the measured differential cross section for  $p + p \rightarrow \gamma + \text{anything}$ ) is inhibited for  $q^2 \geq 33.3 \text{ BeV}^2$ . Since the maximum  $q^2$  available at  $s = 60 \text{ BeV}^2$  is  $q^2 = 34.5 \text{ BeV}^2$ , the suppression of the differential cross section will not be observed except at the very end of the  $q^2$  spectrum.

## V. LEPTON-ANTILEPTON ANNIHILATION INTO HADRONS

Turning finally to process III, we can make the tree graph decomposition shown in Fig. 5a. It is clear that no tree graph can be drawn, for the case in which only hadrons occur in the final state, such that a line of zero virtual mass connects to the photon vertex. The closest we can come to this occurrence is shown in the first tree graph on the right in Fig. 5a in which a single  $\pi$  is produced at the photon vertex.

Since the pion mass is non-zero, however, we expect this contribution to the total cross section  $\sigma_T(q^2)$ , to decrease faster than any power in  $q^2$ . This is, of course, only true if the time like, as well as the space like, elastic form factor is decreasing faster than any power of  $q^2$ , but we have shown in Ref. 3, that if the bootstrap model is accepted, then this, in fact, must be the case. Since the two-pion state is the lightest hadronic state that can be produced, we expect, from Eq. (3), the cross section for  $2\pi$  production to be larger than that for any other particular final hadron state. Furthermore, if the multiplicities of final state particles do not increase faster than any power of  $q^2$ , it follows that  $\sigma_T(q^2)$ , itself, should fall off rapidly in  $q^2$ .

If we restrict process III to those events in which a proton is observed among the final state products, then, in analogy to the variable  $\omega$ , in process I, one can define a variable  $\omega = 2q \cdot p/q^2$  where  $q$  is the photon momentum and  $p$  is the proton momentum. Then it is a natural question to ask whether there is a scaling law for structure functions for process III in terms of the dimensionless variable  $\omega$ . Here we claim the answer is no, as the exponential function in Eq. (1) does not scale. This prediction is in contrast to a result in perturbation theory, of a field theoretic model<sup>8</sup> of pseudoscalar mesons and nucleons, which predicts a very similar behavior for the differential cross sections for processes I and III.

Finally, we note that everything that has been said about the three processes assumed that we were working to the lowest order in electromagnetism. For processes I and II there is no reason to believe this is not valid, but for process III, this may not be the case. In particular, we observe that the cross section for the process  $l^+ l^- \rightarrow \text{hadrons} + \gamma$ , with a real photon emitted in the final state, may eventually dominate the cross section for production of purely hadronic final states. This can be understood in terms of the tree graph in Fig. 5b, in which a zero mass photon connects directly to the virtual photon vertex and thus, by Eq. (3), kills the rapidly decreasing dependence in  $q^2$ . Thus we predict that the ratio

$$\frac{\sigma(q^2)|_{l^+ l^- \rightarrow \text{hadrons}}}{\sigma(q^2)|_{l^+ l^- \rightarrow \text{hadrons} + \gamma}} \quad (24)$$

should go to zero faster than any power in  $q^2$ . This prediction relies, of course, on the assumption that Eqs. (1), (2), and (3) properly describe the hadron  $-\gamma-\gamma$  vertex, for which there is as yet no experimental evidence. A rough estimate of the  $q^2$  value for which the ratio in Eq. (24) should be of order 1 can be obtained for the particular case

$$r = \frac{\sigma(q^2)|_{l^+ l^- \rightarrow p\bar{p}}}{\sigma(q^2)|_{l^+ l^- \rightarrow \pi^0 \gamma}} \quad (25)$$

We estimate the numerator by assuming that at large  $q^2$  the time-like and space-like proton form factors are comparable; we estimate the denominator by using the experimental  $\pi$  decay rate, which should be a good approximation, even for one photon for off-mass-shell, because of Eq. (3) and the fact that the other photon is on the mass-shell. This leads to the value  $q^2 \approx 6 \text{ BeV}^2$  for which  $r$  in Eq. (25) should be comparable to 1. For  $q^2 \approx 6 \text{ BeV}^2$  we predict, then, a surprisingly large rate for production of final state photons compared to the rate for production of a proton-antiproton pair.

## VI. SUMMARY

We have presented a unified model, based on the bootstrap theory of Ref. 2, for three hadronic processes involving high mass virtual photons. Our analysis of these processes is based on the connection, implicit in Eqs. (1), (2), and (3), between slowly varying form factors and internal lines of tree graphs with zero virtual mass. The dominant contributions at large  $q^2$  arise from those tree graphs in which a zero mass internal line can connect correctly to the photon vertex. Thus a peripheral mechanism is established for these processes and a number of interesting predictions are shown to follow.

For the elastic scattering process  $\ell^- p \rightarrow \ell^- p$ , the theory predicts hadronic form factors which decrease faster than any power in  $q^2$  according to Eqs. (1) and (2). For process I,  $\ell^\pm p \rightarrow \ell^\pm +$  hadrons we predict slow  $q^2$  dependence of the structure functions in the deep inelastic region provided the internal line in the tree graph in Fig. 3b can have vanishing virtual mass in the physical region. This constrains the particles emitted backward in the c. m. system to have invariant mass restricted by Eq. (9), and this constraint requires the proton to be emitted forward relative to the incident photon, and, for a given value of  $\omega = 2M_N \nu / Q^2$ , restricts the multiplicities of the final state particles.

For process II,  $pp \rightarrow \ell^+ \ell^- +$  hadrons, we also predict an essentially flat  $q^2$  dependence from the photon vertex because of the peripheral graph in Fig. 4b. However, this graph can only contribute, in the physical region, with  $t = 0$ , if the invariant mass of one of the two groups of particles is less than a nucleon mass, thus requiring the presence of mesons in the final state and leading to the strong prediction that the ratio of the cross section for production of a lepton pair and proton pair over the cross section for production of a lepton pair, a proton pair and a meson should go to zero faster than any power of  $q^2$ . In

addition, we showed that, for fixed  $s$ , the multiplicity of final state mesons produced at the lower vertex in Fig. 4b is strongly dependent on  $q^2$ . For both processes I and II our model is not inconsistent with, although does not predict, a scaling law for the structure functions.

On the other hand, the differential cross sections for process III,  $\ell^+ \ell^- \rightarrow \text{hadrons}$ , is predicted to decrease faster than any power in  $q^2$  and the structure functions cannot scale. Because of the smallness of the pion mass and Eqs. (1), (2), and (3), the cross section for production of a  $\pi^+ \pi^-$  pair is expected to dominate the cross section for the production of any other hadronic state such as a  $p\bar{p}$  pair. Finally we predict that the ratio of the cross section for production of a proton-antiproton pair over the cross section for production of a  $\pi^0$  and a photon should go to zero faster than any power of  $q^2$  and, for  $q^2 \approx 6 \text{ BeV}^2$ , should be of order 1.

## VII. ACKNOWLEDGEMENTS

It is a pleasure to thank Prof. R. Socolow and Dr. D. Levy for their helpful suggestions and critical reading of the manuscript. The hospitality extended to the author by Prof. S. Drell is also gratefully acknowledged.



## FOOTNOTES AND REFERENCES

1. W. Panofsky, Proceedings of the 14th International Conference on High Energy Physics, Vienna (1968).
2. J. Harte, "Off-mass shell theory of the bootstrap and composite particle scattering," Yale University, Hew Haven, Connecticut (1969); to be published in Phys. Rev. 184 (1969).
3. J. Harte, and K. Ong, "Bootstrap prediction for the wide angle proton-proton scattering amplitude," Yale University, New Haven, Connecticut (1969); to be published in Phys. Rev. 184 (1969).
4. J. Bjorken, Report No. SLAC-PUB-510, Stanford Linear Accelerator Center, Stanford University, Stanford, California; to be published.
5. D. Coward, et al., Phys. Rev. Letters 20, 292 (1968).
6. The actual  $q^2$  dependence of the  $W_i(q^2, \nu)$  is quite difficult to determine in this model because Eq. (1) is only correct up to an as yet undetermined multiplicative term with power dependence in the invariant variables. However, since a detailed fit to the elastic nucleon form factor data and large angle proton-proton scattering data seems to be consistent with no power dependent term in the vertex function, we may expect the  $W_i(q^2, \nu)$  to have, at most, a  $1/q^2$  behavior, coming from the integral over  $t$ , for large  $q^2$ .
7. H. Harari, Phys. Rev. Letters 22, 1078 (1969).
8. S. Drell, D. Levy, and Y. Yang, Report No. SLAC-PUB-606, Stanford Linear Accelerator Center, Stanford University, Stanford, California (1969); to be published.

## FIGURE CAPTIONS

1. Illustration of three hadronic processes involving virtual photons.

(a) lepton + proton  $\rightarrow$  lepton + hadrons

(b) proton + proton  $\rightarrow$  lepton pair + hadrons

(c) lepton pair  $\rightarrow$  hadrons.

The dashed, wavy and solid lines refer to leptons, photons and hadrons respectively.

2. Illustration of a general interaction of a photon with hadrons.

3. (a) Tree decomposition of process I. The wavy line refers to the photon, the straight light lines refer to initial and final hadrons, the heavy lines refer to internal lines in the tree graphs, and the circles refer to the vertex in Eq. (1).

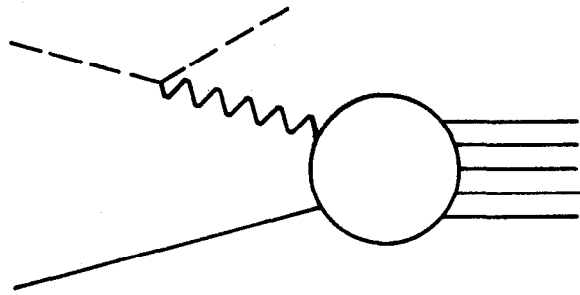
(b) Subclass of tree graphs for process I characterized by a peripheral production mechanism. The open circles can be further decomposed into tree graphs.  $M_1$  and  $M_2$  refer to the invariant masses of the hadrons produced at the lower and upper vertices and  $t$  is the square of the momentum transfer between the photon and the hadrons produced at the upper vertex.

4. (a) Tree decomposition for process II.

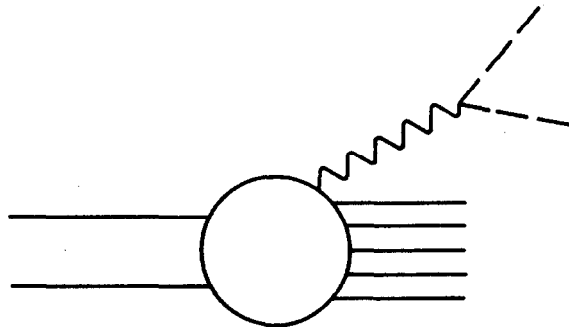
(b) Subclass of tree graphs for process II characterized by a peripheral production mechanism.

5. (a) Tree decomposition for process III.

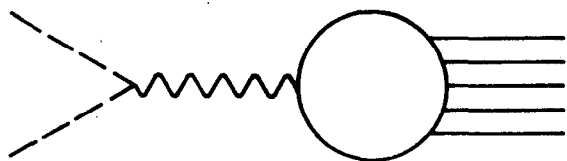
(b) Tree graph for the process  $e^+ e^- \rightarrow \pi^0 \gamma$ .



(a)



(b)



(c)

1384A1

Fig. 1

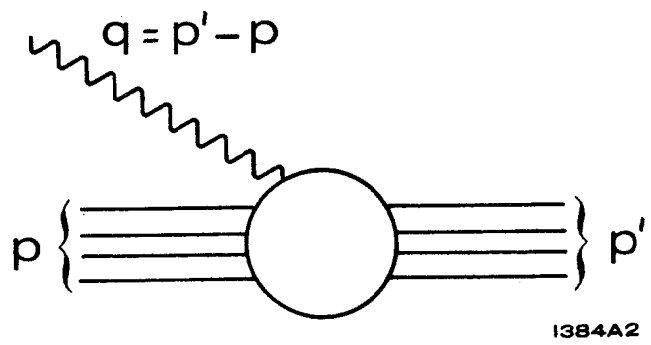


Fig. 2

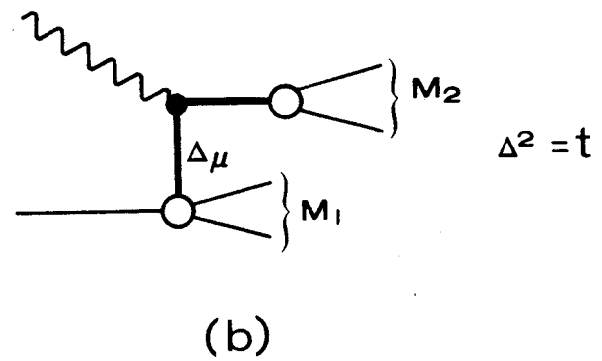
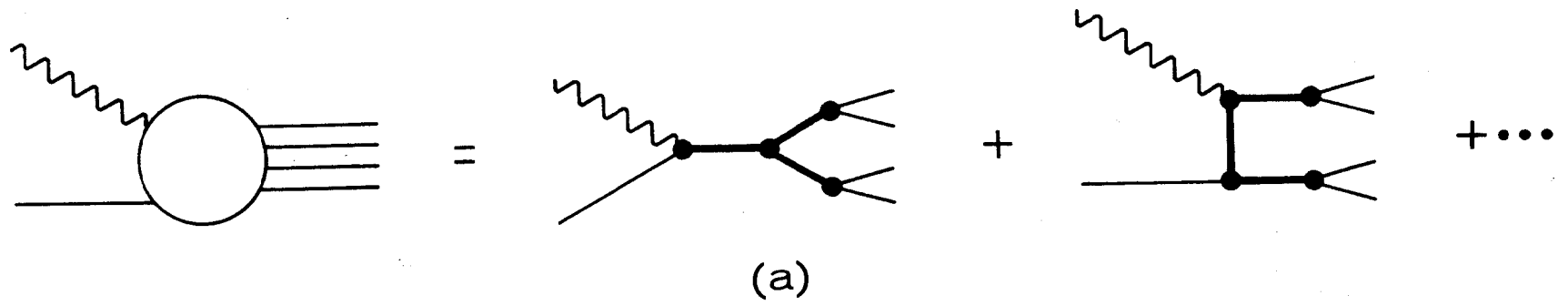
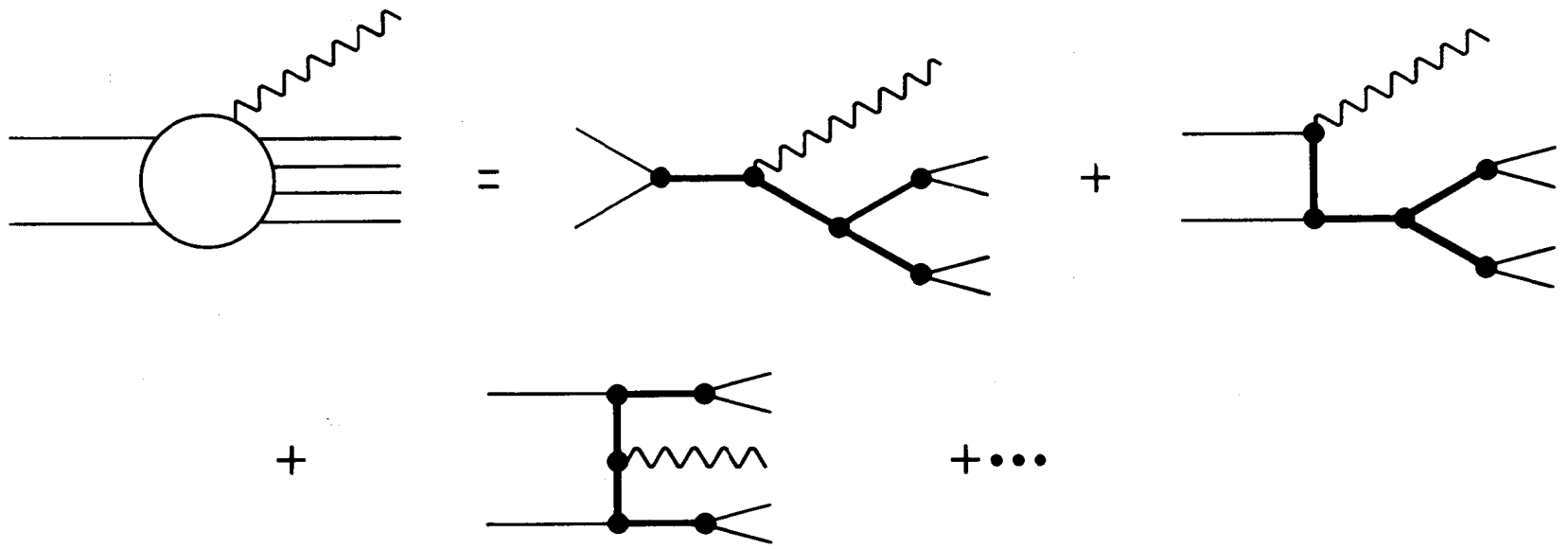
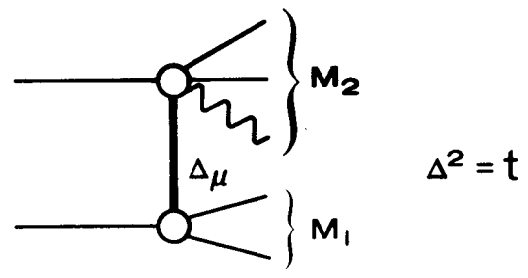


Fig. 3

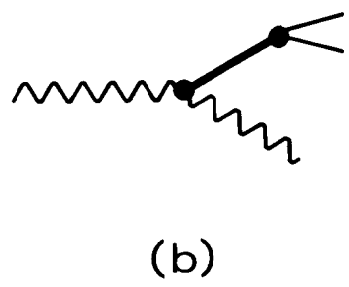
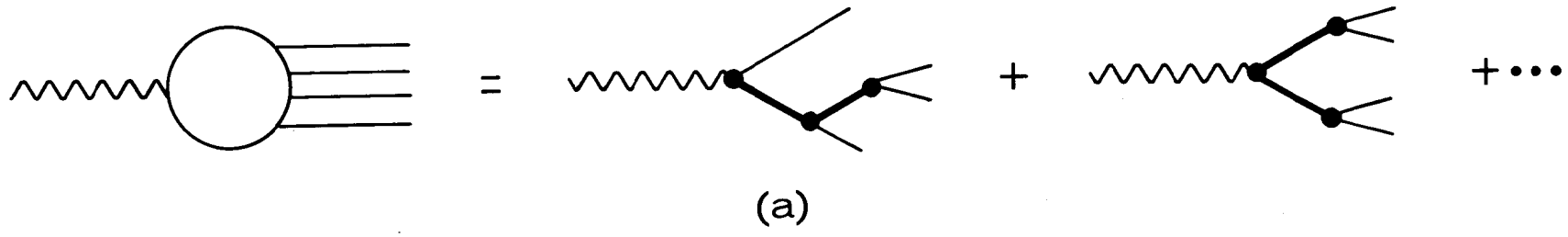


(a)



(b)

Fig. 4



1384A5

Fig. 5